Ferromagnetism in the beta-manganese structure: $Fe_{1.5}Pd_{0.5}Mo_3N$

2004 J. Phys.: Condens. Matter 16 2273

(http://iopscience.iop.org/0953-8984/16/13/008)

INSTITUTE OF PHYSICS PUBLISHING JOURNAL OF PHYSICS: CONDENSED MATTER

J. Phys.: Condens. Matter **16** (2004) 2273–2281 PII: S0953-8984(04)73993-4

Ferromagnetism in the beta-manganese structure: $Fe_{1.5}Pd_{0.5}Mo_3N$

Timothy J Prior[1], **Duc Nguyen-Manh**[2], **Victoria J Couper**[1] **and Peter D Battle**[1,3]

[1] Inorganic Chemistry Laboratory, Oxford University, South Parks Road, Oxford OX1 3QR, UK
[2] Theory and Modelling Department, UKAEA Fusion, Culham Science Centre, Abingdon OX14 3DB, UK

E-mail: peter.battle@chem.ox.ac.uk

Received 5 January 2004
Published 19 March 2004
Online at stacks.iop.org/JPhysCM/16/2273 (DOI: 10.1088/0953-8984/16/13/008)

Abstract

The first example of ferromagnetism in a compound crystallizing with the filled beta-manganese structure is reported. Magnetometry and neutron diffraction show that $Fe_{1.5}Pd_{0.5}Mo_3N$ is ferromagnetic below 160 K, with a saturation magnetization of 2.44 μ_B/formula unit which is associated with the Fe/Pd sublattice. Self-consistent spin-polarized electronic structure calculations, performed within density functional theory, predict an average magnetic moment of 2.93 μ_B/formula unit at $T = 0$ K. The moment is shown to be a result of the fulfilment of a local Stoner criterion on the Fe sites.

1. Introduction

The beta phase of elemental manganese has a crystal structure which is as complex as that of any other metal. The cubic structure has atoms on two distinct sites, the Wyckoff 8c and 12d positions in space group $P4_132$. The former sites (labelled M or I) generate a (10, 3)-a network [1] of Mn atoms and the space within this network is filled by corner-sharing Mn_6 octahedra, (figure 1) with Mn atoms located on the 12d (labelled T or II) sites. The empirical formula of a phase adopting this structure can thus be represented as M_2T_3. β-Mn is the only stable phase of the element which does not show long-range magnetic order at low temperature. It is apparently paramagnetic down to the lowest temperatures measured, in contrast to the antiferromagnetic behaviour ($T_N = 95$ K) exhibited by α-Mn. The electronic behaviour of β-Mn has been studied by a variety of techniques (NMR, specific heat, neutron scattering) but it is still not fully understood, and research is ongoing [2, 3]. It has been suggested relatively recently [3] that it is a quantum spin liquid with antiferromagnetic correlations present between itinerant magnetic moments at the T sites, and that long-range magnetic order is prevented by the presence of geometrical frustration and strong zero-point fluctuations; doping with 10% aluminium

[3] Author to whom any correspondence should be addressed.

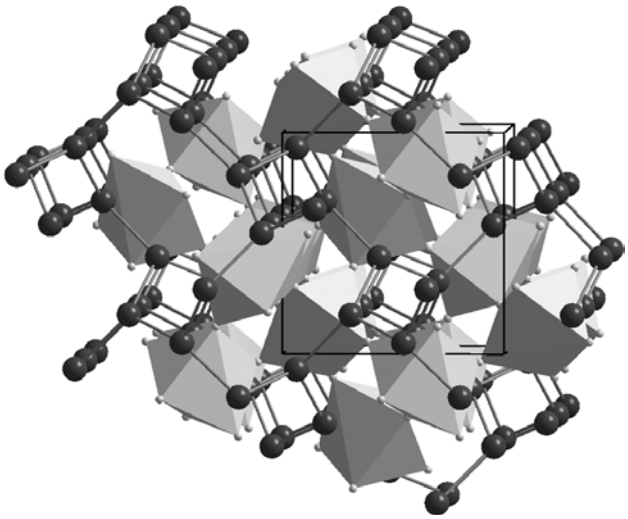

Figure 1. The filled β-Mn structure, M_2T_3X. Space within the (10, 3)-a network of M atoms (black) is filled by corner-sharing T_6X octahedra (grey).

appears to damp the spin fluctuations to create a spin-glass state. It is generally agreed that the behaviour of doped (i.e. alloyed) β-Mn phases is a function of the d-electron concentration and the interatomic distances, but that the spin correlations are always antiferromagnetic.

At the centre of the T_6 octahedra in the β-Mn structure there exists an interstitial site which is large enough to accommodate an electronegative non-metal atom. This site is occupied in a number of 'filled' β-Mn phases M_2T_3X (X = B, C, N) [4] which can be prepared by relatively complex routes involving, in the case of X = N, the ammoniation of oxide precursors [5]. We have recently [6] devised a relatively simple synthesis which has allowed us to extend the known compositional range of these compounds to include, for example, $Ni_{2-x}Co_xMo_3N$, $Ni_{2-x}Pd_xMo_3N$, and $Fe_{2-x}Pd_xMo_3N$. We therefore have the opportunity to control the electron concentration on the M sublattice, and hence the possibility of controlling the electronic properties of the material. More specifically we have the means to introduce a magnetic moment on to the 8c site, non-magnetic in the case of β-Mn itself, and to determine whether the structure is able to support long-range ferromagnetic or antiferromagnetic order in these circumstances; no such order has previously been reported in β-Mn phases. This paper focuses on compositions in the series $Fe_{2-x}Pd_xMo_3N$. We shall show, by a combination of magnetometry and neutron diffraction, that, in contrast to the paramagnetism and spin glass behaviour shown by other compositions which adopt the β-Mn structure, compounds in this series order ferromagnetically at relatively high temperatures (>100 K). We also present calculations based on the tight-binding (TB) linear muffin-tin orbital (LMTO) atomic-sphere approximation (ASA) technique which provide insight into the band structure of these materials and allow us to rationalize our experimental results.

2. Experimental details

2.1. Synthesis

Polycrystalline samples of $Fe_{2-x}Pd_xMo_3N$ were prepared by standard ceramic techniques. Stoichiometric mixtures of the appropriate metal oxides were intimately ground, pelletized and fired under a flow of synthesis gas (about 4.2 $dm^3\ h^{-1}$) for 48 h at 700, and 24 h at 750, 875, and twice at 975 °C, with intermittent regrinding. (Reagent purities: iron oxide (Alfa

Aesar, 99.998%), molybdenum trioxide (Alfa Aesar, 99.9995%), palladium oxide (Johnson Matthey, 99.9%). Synthesis gas: 10% H_2 in N_2 (Air Products).)

In all cases the samples were cooled to room temperature under flowing gas after switching off the furnace. No study of the effects of variation of the cooling rate was carried out. No special handling techniques were applied to samples following their removal from the furnace.

2.2. Characterization

The progress of each synthesis was charted by x-ray powder diffraction using a Philips diffractometer operating with Cu Kα radiation. Relatively high resolution data to be used in quantitative analyses were collected using a Siemens D5000 diffractometer nominally operating with Cu Kα_1 radiation over the angular range $10 \leqslant 2\theta/^\circ \leqslant 125$ with a step size of $\Delta 2\theta = 0.02^\circ$. However, imperfect monochromation introduced a contribution of approximately 2% Kα_2 which was allowed for in the data analysis.

Neutron powder diffraction data were collected on about 4.6 g of $Fe_{1.5}Pd_{0.5}Mo_3N$ using the instrument D 1b at the Institut Laue Langevin, Grenoble, France. D 1b is a high flux, medium resolution instrument operating with a wavelength 2.5219 Å. Data were collected over an angular range $18^\circ \leqslant 2\theta \leqslant 98^\circ$ with a stepsize $\Delta 2\theta = 0.2^\circ$ at 200 and 5 K. Samples were contained within vanadium cans which were mounted in a He cryostat during data collection. Scattering attributable to the cans occurs at $2\theta \approx 72^\circ$ and data in this region were excluded from the analysis. Rietveld refinement [7] of the crystal structures was carried out using the GSAS [8] and FULLPROF [9] suites of programs. Backgrounds were fitted using a shifted Chebyshev polynomial of the first kind. Peak shapes were modelled using a pseudo-Voigt function. In the analysis of the data, three atomic coordinates were varied, along with an isotropic displacement parameter for each crystallographic site.

Thermogravimetric analysis (TGA) was performed using a Rheometric Scientific STA1500 instrument. Samples were loaded into alumina pans and heated under a flow (1.8 $dm^3\ h^{-1}$) of pure oxygen. Nitrogen analysis was performed using a Carlo Erber 1106 CHN analyser.

Magnetic measurements were carried out using a Quantum Design MPMS 5000 SQUID magnetometer. The sample magnetization (M) was measured as a function of temperature ($5 \leqslant T/\mathrm{K} \leqslant 350$) during warm up after cooling to 5 K in either zero field (ZFC) or in the measuring field of 100 Oe (FC). In selected cases, the magnetization was measured as a function of field ($-50 \leqslant H/\mathrm{kOe} \leqslant 50$) after cooling to the measuring temperature in a field of 50 kOe.

Four-probe conductivity measurements were performed using an apparatus constructed within the laboratory. Bars were cut from pellets which were sintered at 800 °C under the synthesis gas. Contacts were attached using silver paint. The conductivity was measured as a function of temperature in the range $80 \leqslant T/\mathrm{K} \leqslant 298$.

2.3. DFT calculations

First-principles spin-polarized electronic structure calculations were performed within the self-consistent tight-binding linear muffin-tin orbital (TB-LMTO) scheme in which the radii of overlapping MT spheres are determined automatically from a full potential construction [10]. Previously this technique has proved to be very efficient for studying the magnetic properties of intermetallic alloys [11–13]. Exchange and correlation contributions to both atomic and crystal potentials were included through the local spin density functional description using the von Barth–Hedin formula [14]. The Brillouin zone integration over **k** space was performed by

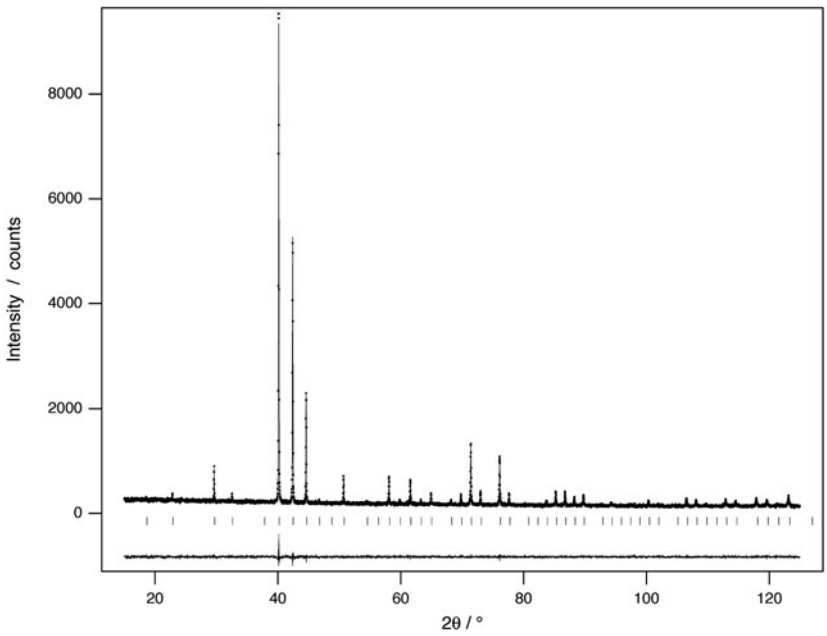

Figure 2. Observed (•), calculated (——) and difference x-ray powder diffraction profiles for $Fe_{1.5}Pd_{0.5}Mo_3N$ at room temperature; tick marks the indicate positions of allowed reflections from the Cu Kα_1 diffraction. The final refinement converged with $R_{wp} = 0.0479$.

means of the improved tetrahedron method using a grid of 272 irreducible **k** points within an accuracy of 10^{-2} mRyd for the total energy per unit cell and 10^{-5} e/au^3 for the charge density. Four formula units of a β-Mn phase M_2T_3X were used to simulate a crystal unit cell for the composition $Fe_{1.5}Pd_{0.5}Mo_3N$.

3. Results

The solid solution $Fe_{2-x}Pd_xMo_3N$ forms in the same cubic structure over the composition range $0.05 \leqslant x \leqslant 2$ when prepared by the reduction–nitridation route described above, albeit sometimes contaminated by molybdenum and Fe_3Mo_3N [15] impurities. However, in the synthesis of the compounds with $0.5 \leqslant x \leqslant 1.5$, the cubic phase was obtained as the predominant component (>99.5%) in product mixtures. The lattice parameter of these cubic phases increases linearly with increasing palladium content, as expected, and there is no evidence for iron–palladium ordering.

The composition $Fe_{1.5}Pd_{0.5}Mo_3N$ has been studied in detail, and an extensive series of measurements of physical properties was carried out. Analysis of x-ray powder diffraction data (figure 2) shows that this compound crystallizes with the filled β-Mn structure with iron and palladium disordered within the (10, 3)-a network of metal atoms; the T(II) sites are occupied exclusively by Mo, with N located at the centre of each Mo_6 octahedron. Crystal data for $Fe_{1.5}Pd_{0.5}Mo_3N$ refined from x-ray diffraction data collected at 300 K are given in table 1.

Rietveld analysis of neutron powder diffraction data collected on D 1b at 200 K affirmed the crystal structure of $Fe_{1.5}Pd_{0.5}Mo_3N$ determined at room temperature by x-ray diffraction, although 0.52(5)% by weight of a phase identified as FePd [16] was present in the sample prepared for neutron diffraction experiments. This was allowed for in the neutron diffraction data analysis, but it was not possible to detect this impurity in the x-ray diffraction data.

Table 1. Atomic positions at 300 K for filled β-Mn nitride $Fe_{1.5}Pd_{0.5}Mo_3N$ derived from x-ray data.

$Fe_{1.5}Pd_{0.5}Mo_3N$: space group $P4_132$, $a_0 = 6.728\,52(12)$ Å, $R_{wp} = 0.0479$						
Atom	Wyckoff position	x	y	z	Occupancy	U_{iso} (Å^2)
Fe	8c	0.0675(3)	0.0675(3)	0.0675(3)	0.75	0.0170(9)
Pd	8c	0.0675(3)	0.0675(3)	0.0675(3)	0.25	0.0170(9)
Mo	12d	1/8	0.2042(2)	0.4542(2)	1	0.0164(4)
N	4a	3/8	3/8	3/8	1	0.016(7)

Chemical analysis and thermogravimetric analysis both confirm full nitrogen occupancy of the 4a interstitial sites; nitrogen analysis (calculated N content 3.19%, measured 3.26%) suggests a composition $Fe_{1.5}Pd_{0.5}Mo_3N_{1.02}$ and complete oxidation of the sample to $FeMoO_4$, MoO_3, and PdO during TGA lead to an increase in mass of 37% (calculated 39%).

Four-probe conductivity measurements indicate that $Fe_{1.5}Pd_{0.5}Mo_3N$ has a resistivity of 2.1×10^{-3} Ω cm at 298 K which varies by less than 1% over the range $80 \leqslant T/\mathrm{K} \leqslant 260$.

SQUID magnetometry data strongly suggest that $Fe_{1.5}Pd_{0.5}Mo_3N$ displays long range ferromagnetic order (figure 3) with $T_c = 160$ K. Measurements of magnetization as a function of applied field at 5 K for $Fe_{1.5}Pd_{0.5}Mo_3N$ are shown in the inset in figure 3(b). The sample saturates in an applied field of about 0.8 T and shows almost no hysteresis about the origin. The saturation magnetization per formula unit is 2.44(2) μ_B (i.e. 1.22 μ_B per 8c site).

Neutron diffraction data collected on D 1b confirmed the presence of long range magnetic order; upon cooling below the Curie point additional Bragg scattering was observed in the diffraction pattern, most notably in two low angle structural reflections, 110 and 111. It was possible to account for this magnetic scattering by locating ferromagnetically ordered spins on the 8c sites of the (10, 3)-a sublattice (figure 4). The moment on each site was refined to a value of 1.20(5) μ_B, which is in excellent agreement with that observed in the magnetometry experiments. A model with ordered spins located on the 12d sites did not improve the fit to the observed diffraction pattern. The compositions $Fe_{0.5}Pd_{1.5}Mo_3N$ and $FePdMo_3N$ were not studied by neutron diffraction, but magnetometry suggests that they also display ferromagnetism, with Curie temperatures of 110 and 160 K, respectively. Their saturation magnetizations are 0.83(1) and 1.73(2) μ_B/formula unit (i.e. 0.415 and 0.865 μ_B per 8c site), demonstrating increasing saturation magnetization with increasing iron content.

A more complete and systematic account of our theoretical studies of the electronic structure and magnetic properties of β-Mn phases M_2Mo_3N (M = Fe, Co, Ni, Pd) will be published elsewhere [17]. Here we only show the results of DFT calculations for the composition $Fe_{1.5}Pd_{0.5}Mo_3N$ which were performed using the experimental values of the lattice constant and atomic parameters shown in the table 1. Self-consistent total energy calculations showed that the ferromagnetic state is more stable than the paramagnetic one by 0.877 eV/unit cell, consistent with the experimental observation of ferromagnetism in $Fe_{1.5}Pd_{0.5}Mo_3N$. A total moment of 11.72 μ_B/unit cell or 2.93 μ_B/formula unit at $T = 0$ K was obtained by DFT calculations. Figure 5(a) shows the calculated total electronic density of states (DOS) where the Fermi energy is positioned at 0.0 eV. At energies less than −15 eV the dominant contribution to the valence band DOS is from N-2s orbitals, while for energies between −8 and −5 eV, the valence band consists of N-2p states strongly hybridized with sp-states of the transition metals (TM) (Mo, Pd and Fe). The main contribution to the total DOS between −5 and 5 eV is from the d-orbitals of the TM atoms. Although the 4d contributions to the Mo DOS at the Fermi level are important, it can clearly be seen from figure 5 that the spin-up

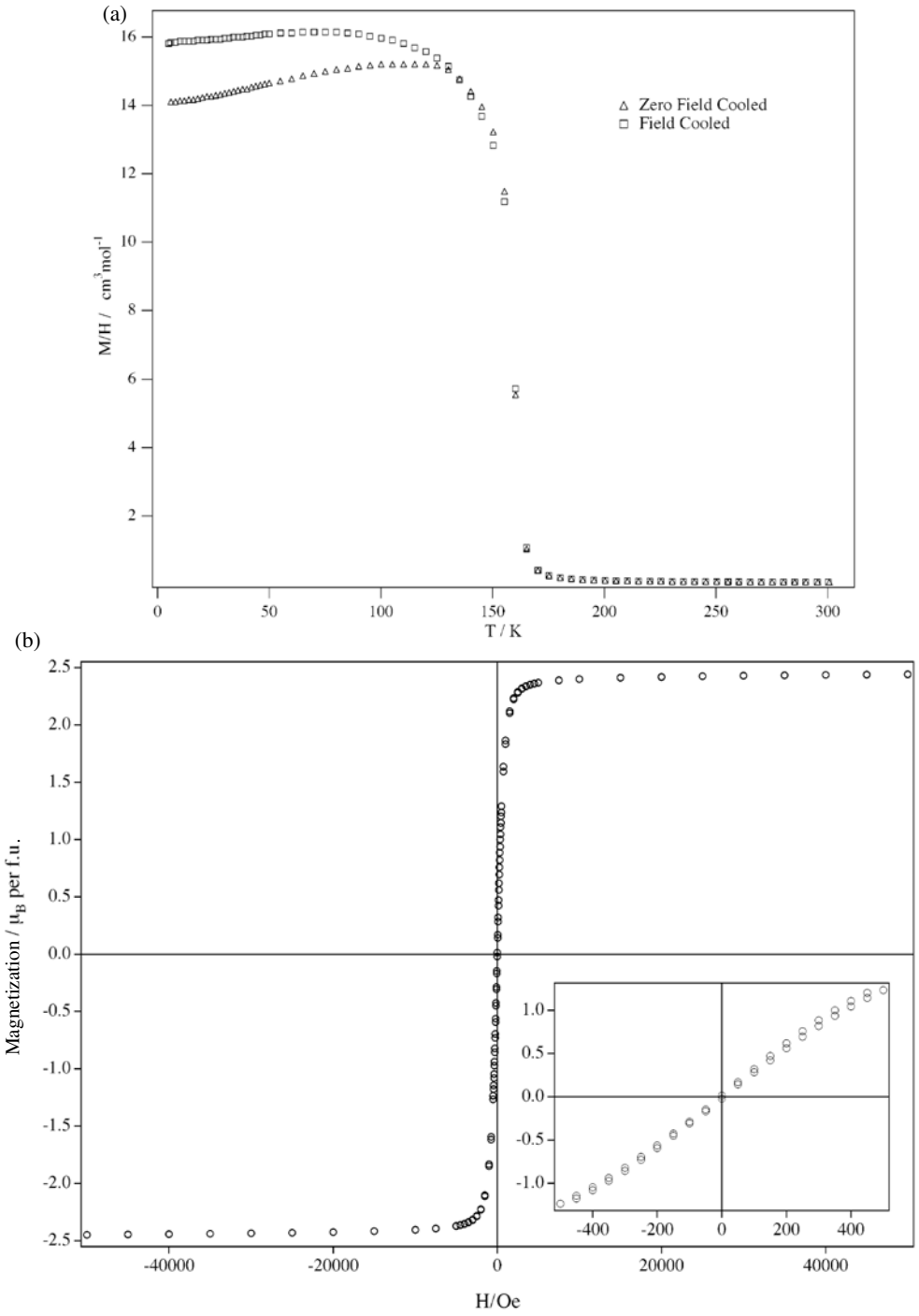

Figure 3. (a) Variation of molar magnetic susceptibility (M/H) with temperature of $Fe_{1.5}Pd_{0.5}Mo_3N$. (b) Magnetization of $Fe_{1.5}Pd_{0.5}Mo_3N$ as a function of applied field at 5 K. The inset shows the region around the origin expanded.

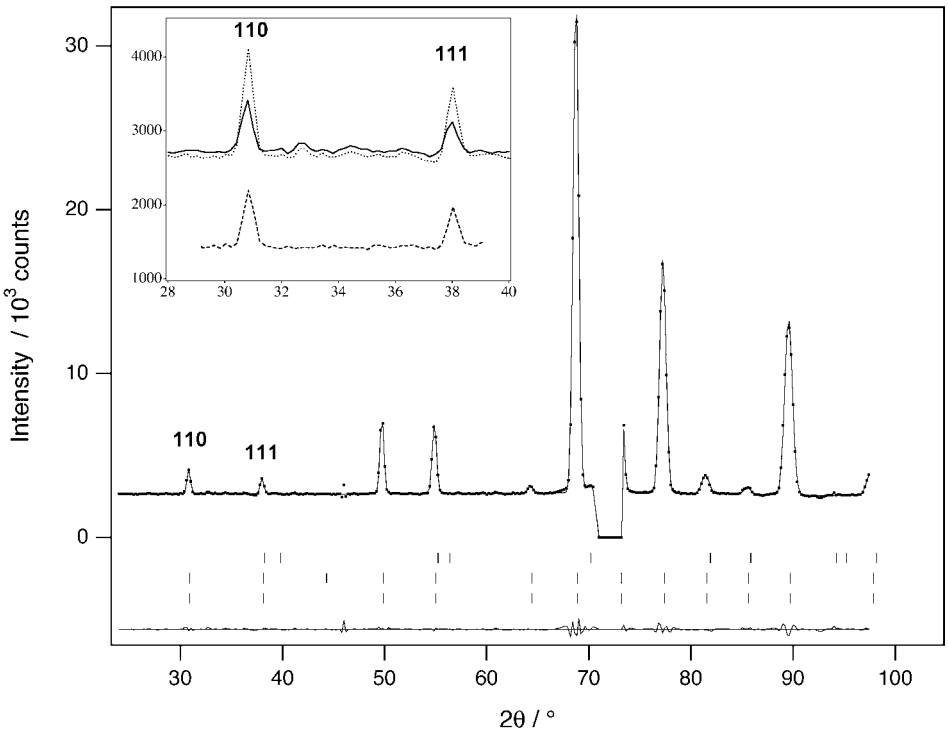

Figure 4. Observed (•), calculated (——) and difference neutron powder diffraction profiles for $Fe_{1.5}Pd_{0.5}Mo_3N$ at 5 K. The lowest tick marks indicate positions of allowed structural reflections; the middle tick marks indicate allowed magnetic reflections; the upper tick marks indicate positions of allowed structural reflections for the FePd impurity. The inset shows data collected at 200 K (solid curve), 5 K (dots) and their difference (lower, dashed curve). Low angle reflections which display additional intensity upon cooling below the Curie point are labelled with their Miller indices.

and spin-down bands are equally populated, and therefore there is no contribution to the bulk magnetization from the Mo (12d) sites. The Pd-4d states are situated essentially in the low energy region, and their contributions at the Fermi energy (figure 5(b)) are almost negligible. Thus calculations show that no local magnetic moment is found at the Pd site. However, the local spin-polarized Fe-3d DOS predicts a strong contribution to the ferromagnetism from the Fe atoms on the 8c sites with an average local magnetic moment of 1.98 μ_B/Fe atom. Finally, the formation of a ferromagnetic state in $Fe_{1.5}Pd_{0.5}Mo_3N$ can be justified in terms of the Stoner criterion [13]. A region of magnetic instability is defined by the condition $N(E_f)I > 1$, where $N(E_f)$ is the local paramagnetic density of states and I is the Stoner exchange interaction. Taking into account that $I \sim 1$ eV for 3d transition metals [18] and using the result $N(E_f) = 2.48$ states eV^{-1}/(Fe atom) from our paramagnetic calculation, we find the Stoner criterion is satisfied and a ferromagnetic ground state is expected.

4. Conclusion

The composition $Fe_{1.5}Pd_{0.5}Mo_3N$, a filled β-Mn phase, has been shown experimentally to be ferromagnetic below 160 K. The measured value of the magnetization (2.44 μ_B/formula unit) is comparable to, although somewhat lower than, the value (2.93 μ_B) predicted by DFT

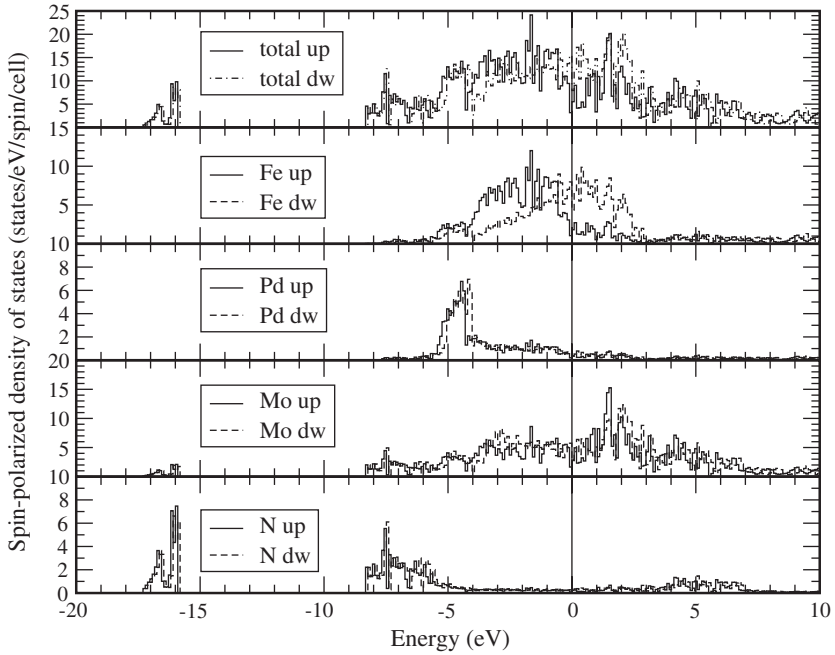

Figure 5. Calculated spin-polarized electronic density of states of $Fe_{1.5}Pd_{0.5}Mo_3N$. Up (solid curve) and down (dashed curve) DOS for total and decomposed Fe, Pd, Mo, N contributions are presented.

calculations. The latter show the ferromagnetic state to be more stable than the paramagnetic state at 0 K, and indicate that the principal contribution to the magnetization comes from the iron atoms (1.98 μ_B/Fe atom), a result which is consistent with both the neutron diffraction data and the Stoner criterion.

The behaviour of this compound is in marked contrast to that of β-Mn itself. The chosen combination of chemical elements leads to a magnetic moment on the 8c (M or I) sites whereas the frustrated local moments in elemental β-Mn are located at the 12d (T or II) sites. This change results in the first observation of ferromagnetism in the β-Mn structure. The extent to which the magnetization and the Curie temperature can be raised by further chemical manipulation is an open question. It is interesting that the presence of Pd facilitates the introduction of Fe into the β-Mn structure; in the absence of the group 10 metal, our reaction conditions generate the η-carbide phase Fe_3Mo_3N.

Acknowledgments

We are grateful to EPSRC for financial assistance and to T Hansen for experimental assistance at ILL. DNM would like to thank D G Pettifor for helpful discussions concerning the β-Mn structure and the Oxford Supercomputing Centre for the provision of facilities.

References

[1] Wells A F 1977 *Three-Dimensional Nets and Polyhedra* (New York: Wiley)
[2] Stewart J R, Rainford B D, Eccleston R S and Cywinski R 2002 *Phys. Rev. Lett.* **89** 186403
Stewart J R and Cywinski R 1999 *Phys. Rev.* B **59** 4305

Sliwko V, Mohn P and Schwarz K 1994 *J. Phys.: Condens. Matter* **6** 6557
[3] Nakamura H, Yoshimoto K, Shiga M, Nishi M and Kakurai K 1997 *J. Phys.: Condens. Matter* **9** 4701
[4] Eibenstein U and Jung W 1997 *J. Solid State Chem.* **133** 21
Jeitschko W, Nowotny H and Benesovsky F 1963 *Monatsh. Chem.* **94** 247
Jeitschko W, Nowotny H and Benesovsky F 1964 *Monatsh. Chem.* **95** 1212
[5] Weil K S, Kumta P N and Grins J 1999 *J. Solid State Chem.* **146** 22
[6] Prior T J and Battle P D 2003 *J. Solid State Chem.* **172** 138
[7] Rietveld H M 1969 *Acta Crystallogr.* **2** 65
[8] Larson A C and von-Dreele R B 1990 *General Structure Analysis System (GSAS)* Los Alamos National Laboratories
[9] Rodriguez-Carvajal J 1990 FULLPROF: a program for Rietveld refinement and pattern matching analysis *Satellite Mtg on Powder Diffraction of the XV Congress of the IUCr (Toulouse, 1990)* p 127 (Abstracts)
Roisnel T and Rodriguez-Carvajal J 2001 *Materials Science Forum* **378–381** 118
[10] Jepsen O and Andersen O K 2000 *The Stuttgart TB-LMTO-ASA Program* Max-Plank-Institut fur Festkorperforschung, Heisenbergstr. 1, D-70569 Stuttgart, Federal Republic of Germany
[11] Neumann A, Nguyen-Manh D, Kjekshus A and Sutton A P 1988 *Phys. Rev.* B **57** 11149
[12] Mukhopadhyay S and Nguyen-Manh D 2002 *Phys. Rev.* B **66** 144408
[13] Nguyen-Manh D and Trambly de Laissardiere G 2003 *J. Magn. Magn. Mater.* **262** 496
[14] von Barth U and Hedin L 1974 *J. Phys. C: Solid State Phys.* **4** 2064
[15] Jackson S K, Layland R C and zur Loye H-C 1999 *J. Alloys Compounds* **291** 94
[16] Fallot M 1938 *Ann. Phys.* **10** 291
[17] Nguyen-Manh D, Prior T J and Battle P D 2004 in preparation
[18] Pettifor D G 1995 *Bonding and Structure of Molecules and Solids* (Oxford: Clarendon)